Published in final edited form as:
Innate Immun. 2013 February ; 19(1): 20–29. doi:10.1177/1753425912447130.

The *LPS2* Mutation in TRIF is Atheroprotective in Hyperlipidemic LDL Receptor Knockout Mice

M. Rachel Richards[1], **Audrey S. Black**[1], **David J. Bonnet**[1], **Grant D. Barish**[2], **Connie W. Woo**[3], **Ira Tabas**[3], **Linda K. Curtiss**[1], and **Peter S. Tobias**[1]

[1]Department of Immunology and Microbial Science, The Scripps Research Institute, La Jolla, CA 92037

[2]Gene Expression Laboratory, the Salk Institute, La Jolla, CA 92037

[3]Department of Medicine, Columbia University, 630 West 168th St., New York, NY 10032

Abstract

Signalling through myeloid differentiation primary response gene 88 (MyD88), an adaptor utilized by all Toll-like receptors (TLR) except TLR3, is pro-atherogenic; however, it is unknown whether signaling through TIR-domain-containing adaptor-inducing interferon-β (TRIF), an adaptor used only by TLRs 3 and 4, is relevant to atherosclerosis. We determined that the *TRIF*^{Lps2} lack-of-function mutation was atheroprotective in hyperlipidemic LDL receptor knockout (LDLr−/−) mice. LDLr−/− mice were crossed with either *TRIF*^{Lps2} or TLR3 knockout mice. After feeding an atherogenic diet for 10–15 weeks, atherosclerotic lesions in the heart sinus and aorta were quantitated. LDLr−/− mice with *TRIF*^{Lps2} were significantly protected from atherosclerosis. *TRIF*^{Lps2} led to a reduction in cytokines secreted from peritoneal macrophages (Mϕ) in response to hyperlipidemia. Moreover, heart sinus valves from hyperlipidemic LDLr−/− *TRIF*^{Lps2} mice had significantly fewer lesional Mϕ. However, LDLr−/− mice deficient in TLR3 showed some enhancement of disease. Collectively, these data suggest that hyperlipidemia resulting in endogenous activation of the TRIF signaling pathway from TLR4 leads to proatherogenic events.

Supplementary Key Words

TRIF; MyD88; TLR3; murine models; inflammation; atherosclerosis

INTRODUCTION

Complications from atherosclerosis are a major contributor to cardiovascular disease, the major cause of morbidity in Western society (1). Atherosclerosis is both a lipid metabolism disorder and a chronic inflammatory disease. Because TLRs play critical roles in activating inflammatory pathways, they provide a mechanistic link between inflammation and atherosclerosis. For example, TLR2 or TLR4 activate pro-inflammatory signaling pathways required for mounting a homeostatic response to infection or sterile injury. However, inappropriate or prolonged activation of these TLRs leads to chronic inflammatory diseases, such as atherosclerosis (2,3).

There is mounting evidence that certain TLRs are pro-atherogenic, although the mechanisms are unclear. Expression of TLR4 message and protein is observed in atherosclerotic plaques

Correspondence: Peter S. Tobias, Ph.D., The Scripps Research Institute, Department of Immunology and Microbial Science, IMM-12, 10550 N. Torrey Pines Rd., La Jolla, CA 92037, USA. Phone: (858) 784-8215, Fax: (858) 784-8239, tobias@scripps.edu.

of humans (4,5). Administration of endotoxin, a mixture of exogenous TLR4 and TLR2 agonists from gram-negative bacteria (6), increases atherosclerosis in rabbits (7). Similarly, activation of TLR2 by Pam3CYSK4 promotes atherosclerosis in mice (8). Experimental deficiency of TLR4 in apoE−/− mice, of TLR2 in LDLr−/− mice, or mutation of TLR4 as in C3H/HeJ mice, leads to less disease (8–11).

Most cell types involved in atherosclerosis express TLRs 2, 3, and 4, as well as MyD88 and TRIF, including at least endothelial cells (ECs), smooth muscle cells and Mϕ (5,12–14). Pro-inflammatory signaling initiated by TLR activation involves two intracellular signaling adaptors, MyD88 and TRIF. Most TLRs, including TLR2 and TLR4, signal through MyD88. TLR3 signals exclusively through TRIF. Only TLR4 signals through both MyD88 and TRIF. Signaling through MyD88 leads to NFκB and MAPK activation, resulting in early up-regulation of inflammatory cytokines such as TNFα, whereas TRIF signaling, in addition to NFκB activation, also activates a subset of type 1 interferon (IFN) response genes, including: IFNβ, RANTES, and IP-10 (15). Although hyperlipidemic ApoE−/− mice deficient for MyD88 are protected from atherosclerosis (9,16), it is unknown whether TRIF deficiency is atheroprotective.

TLRs are activated by both exogenous and endogenous ligands, both of which may play a role in atherosclerosis. Whereas exogenous agonists arise from bacteria or viruses, endogenous agonists arise from host molecules produced as a result of cell death (17) or host pathology (18–21) Hyperlipidemia results in an increase in several candidate endogenous ligands for TLRs generated from host molecules. Candidate endogenous ligands for TLR4 include: heparin sulfate fragments, HMGB1, hyaluronic acid, biglycan, mmLDL (minimally modified low density lipoprotein), and oxidized LDL (oxLDL) (22–25). Hyperlipidemia provides a proatherogenic setting in which TLR may be activated, suggesting a mechanism for TLR activation in atherosclerosis by endogenous agonists.

To explore the role of TRIF in atherosclerosis, we studied LDLr−/− mice expressing the inactive *LPS2* form of the TRIF gene (15). These mice are functionally TRIF deficient due to a point mutation in the carboxyl terminus of the TRIF gene that results in a nonfunctional, truncated protein product. Peritoneal Mϕ isolated from these TRIF-deficient mice do not respond to exogenous TLR3 agonists and have a muted response to TLR4 agonists; however, signaling through the other TLRs, which solely depends on the MyD88 adaptor, is intact (15). These mice are designated $TRIF^{LPS2/LPS2}$. In this report, we show that this TRIF mutation was atheroprotective in hyperlipidemic LDLr−/− mice. We also tested whether mice fed a high fat diet and deficient in both LDLr and TLR3 were protected from atherosclerosis. The effect of TLR3 deficiency was weak, but, on balance, TLR3 deficiency led to more disease.

MATERIALS & METHODS

Animals

All mice were of a *C57BL/6* background. LDLr−/− mice were purchased from Jackson Laboratory (Bar Harbor, ME) and bred in-house. TRIF mutant ($TRIF^{LPS2/LPS2}$) mice, which were generated by ethylnitroso urea mutagenesis of *C57BL/6* mice, were a kind gift from Kasper Hoebe.(15) TLR3 knockout (TLR3−/−) mice on a *C57BL/6* background were obtained from Richard Flavell (26). Double-mutant LDLr−/−$TRIF^{LPS2/LPS2}$ and LDLr−/−TLR3−/− mice were generated in-house. Offspring displayed an apparently normal phenotype and were healthy and fertile. LDLr−/− genotyping was confirmed by PCR, as described (27). The *LPS2* point mutation in the *TRIF* gene was confirmed by sequencing, as described (15). TLR3 deficiency was confirmed in LDLr−/− TLR3−/− mice by assaying for their inability to increase plasma IL-12/IL-23p40 in response to the TLR3 agonist, poly(I:C)

(see below). Mice were weaned at 4 weeks and given *ad libitum* access to standard mouse chow (7019; Harlan Teklad). Age- and sex-matched cohorts were fed a high-fat diet (HFD) *ad libitum* at 8–10 weeks of age. The diet contained 1.25% cholesterol and 15.8% fat (with no added cholate; 94059; Harlan Teklad). Blood samples were collected from fasted animals by retro-orbital puncture using heparin-coated capillary tubes. All mice were housed 4 per cage in autoclaved, filter-top cages with autoclaved water and kept on a 12-hour light/dark cycle. All animal procedures were done in accordance with the Public Health Service (PHS) Policy on Humane Care and Use of Laboratory Animals and The Institutional Animal Care and Use Committee.

Plasma Measurements/ELISAs

Blood samples were centrifuged and plasma was collected and stored at −80°C until use. Enzymatic measurement of total plasma cholesterol was performed using a colorimetric kit (Thermo Electron Corp). Plasma serum amyloid A (SAA) (BioSource) and IL-12/IL-23p40 (R&D Systems) were measured by ELISA. For phenotypic assessment of TLR3 deficiency, mice were injected intraperitoneally (i.p.) with 100 μl of either 100 ng Kdo2-LA (Avanti) or 20 μg poly(I:C) (InvivoGen).

Assessment of Atherosclerosis

After 10 to 15 weeks of consuming a HFD, mice were euthanized, perfused with PBS, fixed with formal-sucrose (4% paraformaldehyde, 5% sucrose in PBS, pH 7.4), and the aortae and hearts dissected. Atherosclerosis was assessed by measuring the *en face* surface area of lesions across the length of the aorta as well as the mean lesion volume within the heart sinus valves, as described (28). For *en face* lesion analysis, aortae were stained with Sudan IV and photographed. The photographs were digitized and total aortic areas and lesion areas calculated using Adobe Photoshop version 7.0 and NIH Scion Image software. The results are reported as a percentage of the total aortic area that contained lesions.

For heart sinus valve lesion analysis, lesion volume was estimated across a fixed distance of the aortic sinus. This method was used instead of lesion cross-section area analysis because the volume analysis is a more accurate method for estimating aortic sinus atherosclerosis in mice (28). Frozen hearts were sectioned on a Leica cryostat, sections were stained with Oil Red O, counterstained with Gill hematoxylin 1 (Fischer Scientific International), photographed, and digitized for lesion analysis. Scoring of valve lesion areas was performed at 4 sites separated by 140 μm for each of the 3 valve cusps individually. Lesion areas found only within the valve cusp were measured. Lesion volume was calculated from an integration of the 4 cross-sectional areas.

Luminex Assay for Inflammatory Cytokines

Unelicited, resident peritoneal Mϕ were harvested from mice fed HFD for 6 weeks and cultured overnight at identical densities (2×10^6 cells/ml) in 6-well dishes (Corning 3516). 0.5 ml of medium (RPMI, 10% FBS) was added to each well. Cell supernatants were collected 24 hours later. Cytokines and chemokines from cell supernatants were quantified using a Bioplex 200 Suspension Array and Procarta assay kits (Panomics/Affymetrix) per manufacturer's instructions.

Immunofluorescence of Heart Sections

Serial heart sections adjacent to selected sections that represented the mean of the volumetric analysis for lesion burden were chosen for immunofluorescent staining. Sections were stained with 1:200 rabbit anti-mouse CD68 IgG (Serotec) and 1:800 DAPI nuclear stain (Invitrogen). Alexa-Fluor 488 conjugated to goat anti-rabbit IgG (Invitrogen) was

applied at 1:500 to visualize the anti-CD68 primary antibody. Slides were examined by confocal microscopy. ImageJ and ImagePro Plus 7.0 software was employed to quantitate CD68-positive staining area and the number of CD68-positive cells that colocalized with DAPI. All quantitations were normalized to the total area of three heart sinus valves per heart section.

Assessment of Necrosis in Heart Lesions

Sections were stained with Harris H&E, and images were viewed and captured with a Nikon Labophot 2 microscope equipped with an Olympus DP25 color digital camera attached to a computerized imaging system with Image-Pro-Plus software (version 3.0; Mediacybernetics). Total intimal lesion area (from internal elastic lamina to the lumen) and acellular/anuclear areas (negative for hematoxylin-positive nuclei) per cross section were quantified by taking the average of 3 sections spaced 10 μm apart beginning at the base of the aortic root. The necrotic core was defined as a clear area that was H&E free. Boundary lines were drawn around these regions, and the area measurements were obtained by image analysis software. A 3,000-μm^2 threshold was implemented to avoid counting very small clear areas frequently observed in H&E-stained sections that likely do not represent substantial areas of necrosis.

Statistical analysis

All scatter plots are expressed with the mean ± standard error. Atherosclerosis data were analyzed by the unpaired Student's *t* test. A value of $p<0.05$ was considered significant.

EXPERIMENTAL RESULTS

Attenuated TLR-Induced Inflammation in Normolipidemic LDLr−/−TRIF$^{LPS2/LPS2}$ Mice

We confirmed the phenotype of the chow-fed LDLr−/−TRIF$^{LPS2/LPS2}$ mice by assessing levels of plasma inflammatory markers in response to the TLR4 or TLR3 exogenous agonists, Kdo2-LA or poly(I:C), respectively. The plasma levels of SAA 24 hours after i.p. injection of 100 ng Kdo2-LA were significantly lower in LDLr−/−TRIF$^{LPS2/LPS2}$ mice compared to LDLr−/− mice, $p<0.01$ (Fig. 1A). Because TLR3 also signals through TRIF, we examined the effects of exogenous TLR3 activation on IL-12/IL-23p40 production, activated in response to TLR3 agonist administration. Normolipidemic LDLr−/− or LDLr−/−TRIF$^{LPS2/LPS2}$ mice were i.p. injected with 20 μg of poly(I:C) and plasma was collected 4 hours later. As expected, poly(I:C) injection increased plasma levels of IL12/IL23p40 in LDLr−/− mice but had no effect on LDLr−/− TRIF$^{LPS2/LPS2}$ mice (Fig. 1B). Thus, the TRIF pathway was functionally deficient in the LDLr−/− TRIF$^{LPS2/LPS2}$ mice that were used in these studies.

Reduced Inflammation in Peritoneal Mφ from Hyperlipidemic LDLr−/−TRIF$^{LPS2/LPS2}$ Mice

Because TRIF is involved in stimulating inflammatory pathways, we predicted inflammation might be suppressed in LDLr−/−TRIF$^{LPS2/LPS2}$ mice in response to hyperlipidemia. Supernatants of unelicited, resident Mϕ harvested from LDLr−/− and LDLr−/−TRIF$^{LPS2/LPS2}$ mice fed HFD for 6 weeks were examined for inflammatory cytokines. No exogenous agonist was administered to these HFD-fed mice. As expected, hyperlipidemia was induced in these mice as indicated by elevated levels of total plasma cholesterol, which were similar in both LDLr−/− and LDLr−/− TRIF$^{LPS2/LPS2}$ mice (1073±32 vs. 1028±64 mg/dl). All the cytokines assessed were markedly suppressed in macrophage supernatants from HFD-fed LDLr−/−TRIF$^{LPS2/LPS2}$ mice (Fig. 2). These results indicate that inflammation observed in response to HFD is attenuated in resident peritoneal Mϕ of LDLr−/−TRIF$^{LPS2/LPS2}$ mice.

Reduced Lesion Burden in LDLr−/−TRIF$^{LPS2/LPS2}$ Mice

Because TRIF activates inflammatory pathways and chronic inflammation can be proatherogenic, we predicted that TRIF inactivation would result in reduced atherosclerosis. To determine the effects of *TRIF*^{LPS2} mutation on atherosclerosis, we assessed lesion burden in cohorts of age-matched LDLr−/− or LDLr−/−TRIF$^{LPS2/LPS2}$ males, fed a HFD for 12 or 15 weeks.

Although weights of 9-week-old, age-matched, male LDLr−/− mice were similar to LDLr−/−TRIF$^{LPS2/LPS2}$ mice at baseline, the LDLr−/− mice gained weight faster than LDLr−/−TRIF$^{LPS2/LPS2}$ mice, as evidenced by a significant weight difference at 6, 12 and 15 weeks of HFD (Supp. Table 1). However, there were no differences between total plasma cholesterol following consumption of the HFD, regardless of the time point examined (Supp. Table 1).

There were significant reductions in lesion burden in aortae of LDLr−/−TRIF$^{LPS2/LPS2}$ male mice at 15 weeks (Fig. 3B) and in the sinus valves of the hearts of LDLr−/−TRIF$^{LPS2/LPS2}$ males at both 12 and 15 weeks (Fig. 3B). Careful examination of potential relationships between lesion burden in hearts or aortae and weights revealed no significant correlations at either time point (Supp. Fig. 1).

Decreased Accumulation of Mφ in Heart Sinus Valves Lesions in Hyperlipidemic LDLr−/−TRIF$^{LPS2/LPS2}$ Mice

Next, we assessed the effect of the LPS2 mutation on Mϕ accumulation in the heart sinus valves of LDLr−/− mice fed HFD for 12 weeks. The central section of the heart sinus analyzed for lesion burden was selected for analysis of Mϕ accumulation. The selected sections were stained with anti-mouse CD68 to identify Mϕ, and DAPI, a nuclear marker, to identify individual cells. A significant decrease in both CD68-positive staining area and CD68-positive staining cell number was observed in hearts of HFD-fed LDLr−/−TRIF$^{LPS2/LPS2}$ mice as compared with LDLr−/− mice (Fig. 4). Notably, the LDLr−/−TRIF$^{LPS2/LPS2}$ hearts also had significantly less lesion burden (Fig. 3). Morphometric lesion analysis revealed no significant differences in percent necrotic core area between LDLr−/− and LDLr−/−TRIF$^{LPS2/LPS2}$ hearts (Supp. Fig. 2), suggesting no overall changes in the levels of Mϕ cell death between LDLr−/− and LDLr−/−TRIF$^{LPS2/LPS2}$ sinus valve lesions.

Atherosclerosis in LDLr−/−TLR3−/− Mice

Because TRIF signals through TLR3, we determined if deletion of TLR3 in LDLr−/− mice was atheroprotective in response to hyperlipidemia. To phenotype the LDLr−/−TLR3−/− mice, plasma from cohorts of chow-fed, age-matched males was assayed for plasma IL-12/IL-23p40 levels in response to i.p. administration of 20 μg poly(I:C), an exogenous TLR3 agonist. LDLr−/− mice treated with poly(I:C) had increased plasma levels of IL-12/IL-23p40 compared to mice treated with saline (Supp. Fig. 3). As expected, LDLr−/−TLR3−/− mice treated with poly(I:C) did not exhibit increased plasma levels of IL-12/IL-23p40, compared to LDLr−/−TLR3−/− mice treated with saline.

These cohorts of mice were then fed the HFD beginning at 9 weeks of age to examine differences in lesion burden. Weights of the two groups were similar at baseline and following 10 or 14 weeks of HFD consumption (Supp. Table 2). Total cholesterol levels of LDLr−/−TLR3−/− mice were similar to that of LDLr−/− mice at baseline and following HFD feeding, except for a reduction in LDLr−/−TLR3−/− mice at 10 weeks (Supp. Table 2). Compared with LDLr−/− mice, lesion burden was certainly not decreased in male LDLr−/−TLR3−/− mice fed a HFD for 10 or 14 weeks in either heart sinus valves or aortae (Fig. 5). Depending on the duration of high fat diet consumption, there was a slight but significant

increase in lesion burden in the aortae of the LDLr−/− TLR3−/− mice at both time points as well as an increase in lesion volume in the hearts of the mice.

DISCUSSION

TRIF Deficiency Diminishes Atherosclerosis in the Context of a High Fat Diet

Our principal conclusion from this work is that in the context of LDLr−/− mice consuming a high fat diet for 12 to 15 weeks in the absence of an administered TLR agonist, a deficiency of TRIF diminishes aortic and heart sinus lesion development.

TRIF Signaling and Production of Inflammatory Cytokines

TRIF deficiency was atheroprotective without changes in total plasma cholesterol. Although there was reduced body weight in LDLr−/−TRIF$^{LPS2/LPS2}$ mice upon consumption of the HFD, there was no correlation between body weight and lesion burden in either hearts or aortae, suggesting that the decrease in lesion burden was not dependent on weight differences (Supp. Fig. 1). However, levels of inflammatory cytokines secreted by unelicited, peritoneal Mϕ from hyperlipidemic LDLr−/−TRIF$^{LPS2/LPS2}$ mice were significantly lower (Figure 2). The decreased inflammatory phenotype of LDLr−/−TRIF$^{LPS2/LPS2}$ mice fed the HFD provides a plausible mechanism for the decrease we observed in lesion burden.

Cytokine expression was suppressed in LDLr−/−TRIF$^{LPS2/LPS2}$ mice despite wild-type expression of MyD88. In addition to up-regulation of type I interferons, the TRIF signaling pathway also activates the NFκB pathway (29). Therefore, it is likely that these NFκB-dependent genes require both TRIF and MyD88 for full activation, at least in response to the endogenous ligands produced by hyperlipidemia. The requirement of both MyD88 and TRIF to mount a full inflammatory response may explain why SAA levels were inhibited in plasma from LDLr−/− TRIF$^{LPS2/LPS2}$ mice injected with Kdo2-LA (Figure 1).

Deficiency of MyD88 also causes elimination of atherosclerosis (9,16). These reports show a greater effect of MyD88 deficiency than we observe, but the fact that their experiments were done using apoE−/− MyD88−/− mice cofounds a direct comparison.

TRIF Deficiency Decreased Macrophage Accumulation in Heart Sinus Lesions

We observed a decrease in CD68+ Mϕ in the sinus lesions of hyperlipidemic, LDLr−/−TRIF$^{LPS2/LPS2}$ mice. This correlated with a significant decrease in lesion burden, suggesting that the decrease in Mϕ in the heart contributes to reduced atherosclerosis. Decreased recruitment of monocytes to lesion prone areas seems the likely explanation for the lesser number of Mϕ in the heart. Increased cell death could also lead to the reduction of Mϕ in heart sinus lesions. This possibility is less likely, however, because no differences in the amount of necrosis in heart lesions were observed between the LDLr−/− and LDLr−/−TRIF$^{LPS2/LPS2}$ mice (Supp. Fig. 4).

TRIF Promotes Atherosclerosis via a TLR3-Independent Mechanism

Collectively, our data show that in HFD-fed LDLr−/− mice, signaling through TRIF by endogenous agonists are pro-atherogenic. As far as is known, TRIF signaling is activated only in response to TLR4 and TLR3 ligands. Because we found that TLR3 deletion did not reduce lesion burden, we conclude that TRIF signaling through another receptor, most likely TLR4 mediates TRIF's atherogenic activity in hyperlipidemic LDLr−/− mice.

Conclusion Summary

Because atherosclerosis is a chronic inflammatory disease of the vasculature, defining the pathways by which that inflammation is initiated is important for a basic understanding of the disease as well as future strategies that might ameliorate the condition. In this work we have focused on the role of a particular inflammatory pathway initiated by activation of TLR4 and TLR3, specifically the TRIF pathway. Using mice deficient in TRIF, we observed a diminution of atherosclerotic disease in the disease model using mice also deficient in the low density lipoprotein receptor fed a high fat diet. Using the same model we also found that mice deficient in TLR3 did not have less disease; they showed a slight increase in disease. Thus, we conclude that signaling initiated by TLR4 transmitted intracellularly through TRIF promotes proatherosclerotic inflammatory events. Whether it is possible to ameliorate atherosclerosis in mice or humans through manipulation of this pathway cannot be tested inasmuch as there are no drugs as yet which target this specific pathway.

While there is no other study of TRIF deficiency in atherosclerosis, the role of TLR3 has been reported in two publications, with variable approaches and variable results. Cole, et al. studied ApoE−/− mice fed a standard chow diet. (30) They observed that TLR3 deficiency led to diminished lesions in the aortic sinus. They also observed that administration of the TLR3 agonist poly(I:C) diminished neointimal thickening in a TLR3 dependent manner. Zimmer, et al also studied ApoE−/− mice, but fed them an atherogenic western diet containing 21% fat, 19.5% casein, and 1.5% cholesterol. (31) They observed that administration of poly(I:C) enhanced aortic sinus lesion formation. They also observed a number of pathologic effects of poly(I:C) on endothelial cell function that were dependent on intact TLR3 function. We tentatively hypothesize that the differences in results observed by Cole, et al., Zimmer, et al., and ourselves are probably attributable to the difference in diets fed as well as the strains of mice used. Further work will be needed to identify the relevant variables and to understand the mechanisms involved.

Supplementary Material

Refer to Web version on PubMed Central for supplementary material.

Acknowledgments

This study was supported by Fellowship AHA 0825013F (to M.R. Richards), NIH grant HL088093 (to L.K. Curtiss), CIHR Fellowship-FAH (to C. Woo), and NIH grants HL087123 and HL075662 (to I. Tabas). The authors wish to thank Karen McKeon for technical assistance, Kasper Hoebe for the TRIF-deficient mice, and Anna Meyers and Barbara Parker for administrative assistance. This is the Scripps Research Institute manuscript no. 20466 (Department of Immunology & Microbiology Science).

Abbreviations

MyD88	Myeloid differentiation primary response gene 88
TLR	Toll-like receptors
TIR	Toll/Interleukin-1 Receptor-Like
TRIF	TIR-domain-containing adaptor-inducing interferon-β
LDLr−/−	LDL receptor knockout
Mϕ	macrophages
ECs	endothelial cells

HFD	high-fat diet
LPS	lipopolysaccharide
TNFα	tumor necrosis factor alpha
RANTES	Regulated upon Activation Normal T Cell-Expressed and Secreted
IP-10	Interferon Inducible Protein-10
NFκB	Nuclear Factor Kappa B
MAPK	Mitogen activated protein kinase
IFN	interferon
IL-12/IL-23p40	Interleukin 12 and Interleukin 23, 40 kDa MW subunit
Kdo2-LA	poly(I:C), Di[3-deoxy-D-manno-octulosonyl]-lipid A
DAPI	4’,6-diamidino-2-phenylindole
SAA	serum amyloid A
mmLDL	minimally modified LDL
oxLDL	oxidized LDL

References

1. Minino AM, Xu J, Kochanek KD, Tejada-Vera B. Death in the United States. NCHS Data Brief. 2009; 26:1–8. [PubMed: 20018136]
2. Curtiss LK, Tobias PS. The toll of Toll-like receptors, especially toll-like receptor 2, on murine atherosclerosis. Curr Drug Targets. 2007; 8:1230–1238. [PubMed: 18220700]
3. Frantz S, Ertl G, Bauersachs J. Mechanisms of disease: Toll-like receptors in cardiovascular disease. Cardiovasc Med. 2007; 4:444–454.
4. Edfeldt K, Swedenborg J, Hansson GK, et al. Expression of toll-like receptors in human atherosclerotic lesions: a possible pathway for plaque activation. Circulation. 2002; 105:1158–1161. [PubMed: 11889007]
5. Xu XH, Shah PK, Faure E, et al. Toll-like receptor-4 is expressed by macrophages in murine and human lipid-rich atherosclerotic plaques and upregulated by oxidized LDL. Circulation. 2001; 104:3103–3108. [PubMed: 11748108]
6. Hirschfeld M, Ma Y, Weis JH, et al. Cutting Edge: Repurification of Lipopolysaccharide Eliminates Signaling Through Both Human and Murine Toll-Like Receptor 2. J Immunol. 2000; 165:618–622. [PubMed: 10878331]
7. Lehr HA, Sagban TA, Ihling C, et al. Immunopathogenesis of atherosclerosis: endotoxin accelerates atherosclerosis in rabbits on hypercholesterolemic diet. Circulation. 2001; 104:914–920. [PubMed: 11514379]
8. Mullick AE, Tobias PS, Curtiss LK. Modulation of atherosclerosis in mice by Toll-like Receptor 2. J Clin Invest. 2005; 115:3149–3156. [PubMed: 16211093]
9. Michelsen KS, Wong MH, Shah PK, et al. Lack of Toll-like receptor 4 or myeloid differentiation factor 88 reduces atherosclerosis and alters plaque phenotype in mice deficient in apolipoprotein E. Proc Natl Acad Sci U S A. 2004; 101:10679–10684. [PubMed: 15249654]
10. Paigen B. Genetics of responsiveness to high-fat and high-cholesterol diets in the mouse. Am J Clin Nutr. 1995; 62:458S–462S. [PubMed: 7625360]
11. Higashimori M, Tatro JB, Moore KJ, et al. Role of Toll-Like Receptor 4 in Intimal Foam Cell Accumulation in Apolipoprotein E-Deficient Mice. Arterioscler Thromb Vasc Biol. 2011; 31:50–57. [PubMed: 20966403]

12. Dunzendorfer S, Lee HK, Soldau K, et al. Toll-like receptor 4 functions intracellularly in human coronary artery endothelial cells: roles of LBP and sCD14 in mediating LPS-responses. FASEB J. 2004; 18:1117–1119. [PubMed: 15132988]
13. Lloyd-Jones KL, Kelly MM, Kubes P. Varying Importance of Soluble and Membrane CD14 in Endothelial Detection of Lipopolysaccharide. J Immunol. 2008; 181:1446–1453. [PubMed: 18606699]
14. Baiersdörfer M, Schwarz M, Seehafer K, et al. Toll-like receptor 3 mediates expression of clusterin/apolipoprotein J in vascular smooth muscle cells stimulated with RNA released from necrotic cells. Exp Cell Res. 2010; 316:3489–3500. [PubMed: 20692254]
15. Hoebe K, Du X, Goode J, Mann N, et al. *Lps2*: a new locus required for responses to lipopolysaccharide, revealed by germline mutagenesis and phenotypic screening. J Endotoxin Res. 2003; 9:250–255. [PubMed: 12935356]
16. Bjorkbacka H, Kunjathoor VV, Moore KJ, et al. Reduced atherosclerosis in MyD88-null mice links elevated serum cholesterol levels to activation of innate immunity signaling pathways. Nat Med. 2004; 10:416–421. [PubMed: 15034566]
17. Lichtnekert J, Vielhauer V, Zecher D, et al. Trif is not required for immune complex glomerulonephritis: dying cells activate mesangial cells via Tlr2/Myd88 rather than Tlr3/Trif. Am J Physiol - Renal Physiol. 2009; 296:F867–F874. [PubMed: 19158348]
18. Van Noort, JM.; Bsibsi, M. Toll-like receptors in the CNS: implications for neurodegeneration and repair. In: Joost Verhaagen, EMH., editor. Progress in Brain Research Neurotherapy: Progress in Restorative Neuroscience and Neurology. Elsevier; 2009. p. 139-148.
19. Smith KD. Toll-like receptors in kidney disease. Curr Opin Nephrol Hypertens. 2009; 18(3):189–196. [PubMed: 19352178]
20. Mkaddem SB, Bens M, Vandewalle A. Differential activation of Toll-like receptor-mediated apoptosis induced by hypoxia. Oncotarget. 2010; 1(8):741–750. [PubMed: 21321383]
21. Kono DH, Haraldsson MK, Lawson BR, et al. Endosomal TLR signaling is required for antinucleic acid and rheumatoid factor autoantibodies in lupus. Proc Natl Acad Sci U S A. 2009; 106:12061–12066. [PubMed: 19574451]
22. Curtiss LK, Tobias PS. Emerging role of Toll-like receptors in atherosclerosis. J Lipid Res. 2009; 50:S340–S345. [PubMed: 18980945]
23. Miller YI, Viriyakosol S, Binder CJ, et al. Minimally modified LDL binds to CD14, induces macrophage spreading via TLR4/MD-2, and inhibits phagocytosis of apoptotic cells. J Biol Chem. 2003; 278:1561–1568. [PubMed: 12424240]
24. Stewart CR, Stuart LM, Wilkinson K, et al. CD36 ligands promote sterile inflammation through assembly of a Toll-like receptor 4 and 6 heterodimer. Nat Immunol. 2010; 11:155–161. [PubMed: 20037584]
25. Seimon TA, Nadolski MJ, Liao X, et al. Atherogenic lipids and lipoproteins trigger CD36-TLR2-dependent apoptosis in macrophages undergoing endoplasmic reticulum stress. Cell Metab. 2010; 12(5):467–482. [PubMed: 21035758]
26. Alexopoulou L, Holt AC, Medzhitov R, et al. Recognition of double-stranded RNA and activation of NF-kappaB by toll-like receptor 3. Nature. 2001; 413:732–738. [PubMed: 11607032]
27. Schiller NK, Kubo N, Boisvert WA, et al. Effect of γ-irradiation and bone marrow transplantation on atherosclerosis in LDL receptor-deficient mice. Arterioscler Thromb Vasc Biol. 2001; 21:1674–1680. [PubMed: 11597944]
28. Schiller NK, Black AS, Bradshaw GP, et al. Participation of macrophages in atherosclerotic lesion morphology in $LDLr^{-/-}$ mice. J Lipid Res. 2004; 45:1398–1409. [PubMed: 15175354]
29. Yamamoto M, Sato S, Hemmi H, et al. Role of adaptor TRIF in the MyD88-Independent Toll-like receptor signaling pathway. Science. 2003; 301:640–643. [PubMed: 12855817]
30. Cole JE, Navin TJ, Cross AJ, et al. Unexpected protective role for Toll-like receptor 3 in the arterial wall. Proc Natl Acad Sci U S A. 2011; 108:2372–2377. [PubMed: 21220319]
31. Zimmer S, Steinmetz M, Asdonk T, et al. Activation of endothelial toll-like receptor 3 impairs endothelial function. Circ Res. 2011; 108:1358–1366. [PubMed: 21493895]

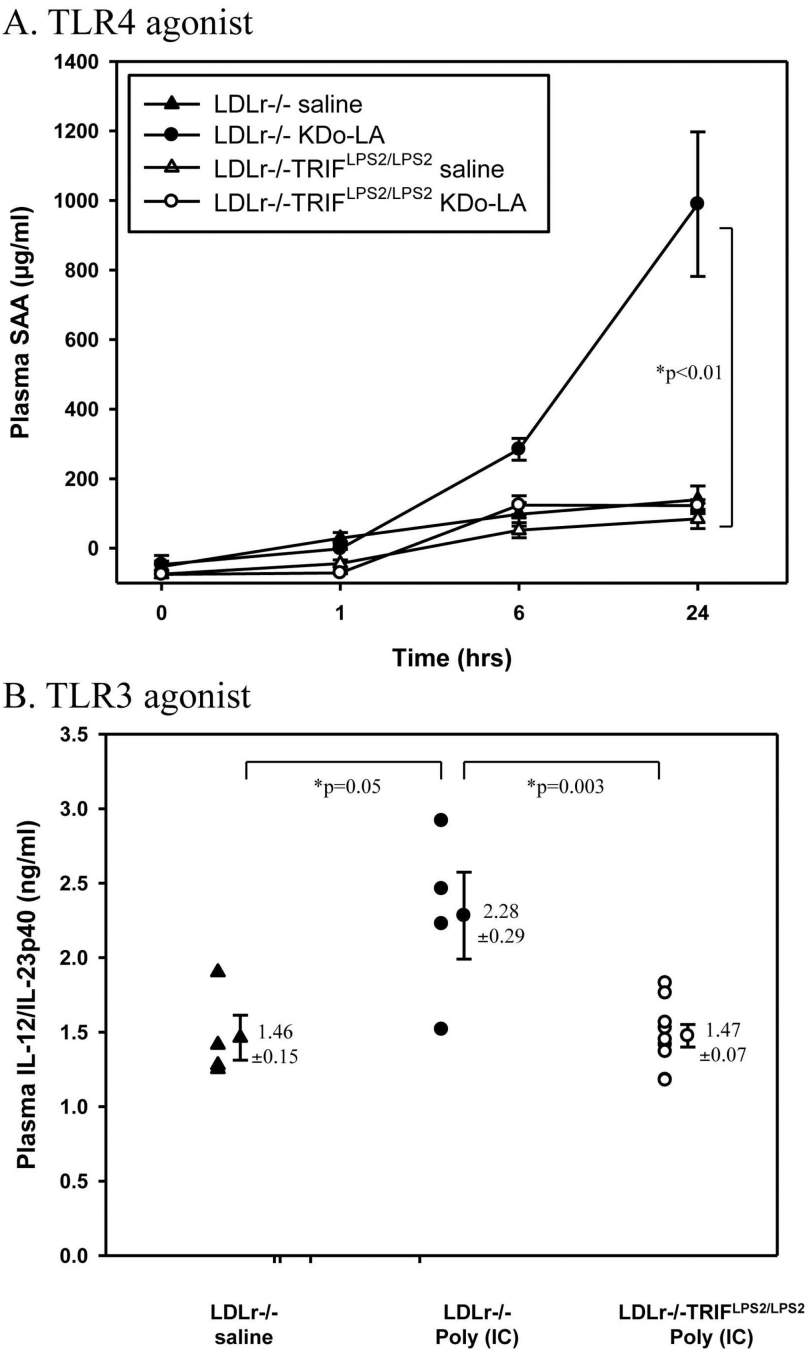

Figure 1. LDLr−/−TRIF$^{LPS2/LPS2}$ Mice Plasma Response to Exogenous TLR4 or TLR3 Agonists

Groups of chow-fed male LDLr−/− (n=4) or LDLr−/−TRIF$^{LPS2/LPS2}$ mice (n=9) were i.p. injected with saline, 100 ng of Kdo2-LA (TLR4 agonist, A) or 20 µg poly(I:C) (TLR3 agonist, B). Plasma was collected at baseline, 1, 6, and 24 hours post-injection for Kdo2-LA, and 4 hours post-injection for poly(I:C). Total plasma SAA in responses to Kdo2-LA (A), or total plasma IL-12/IL-23p40 in responses to poly(I:C) (B), were measured by ELISA.

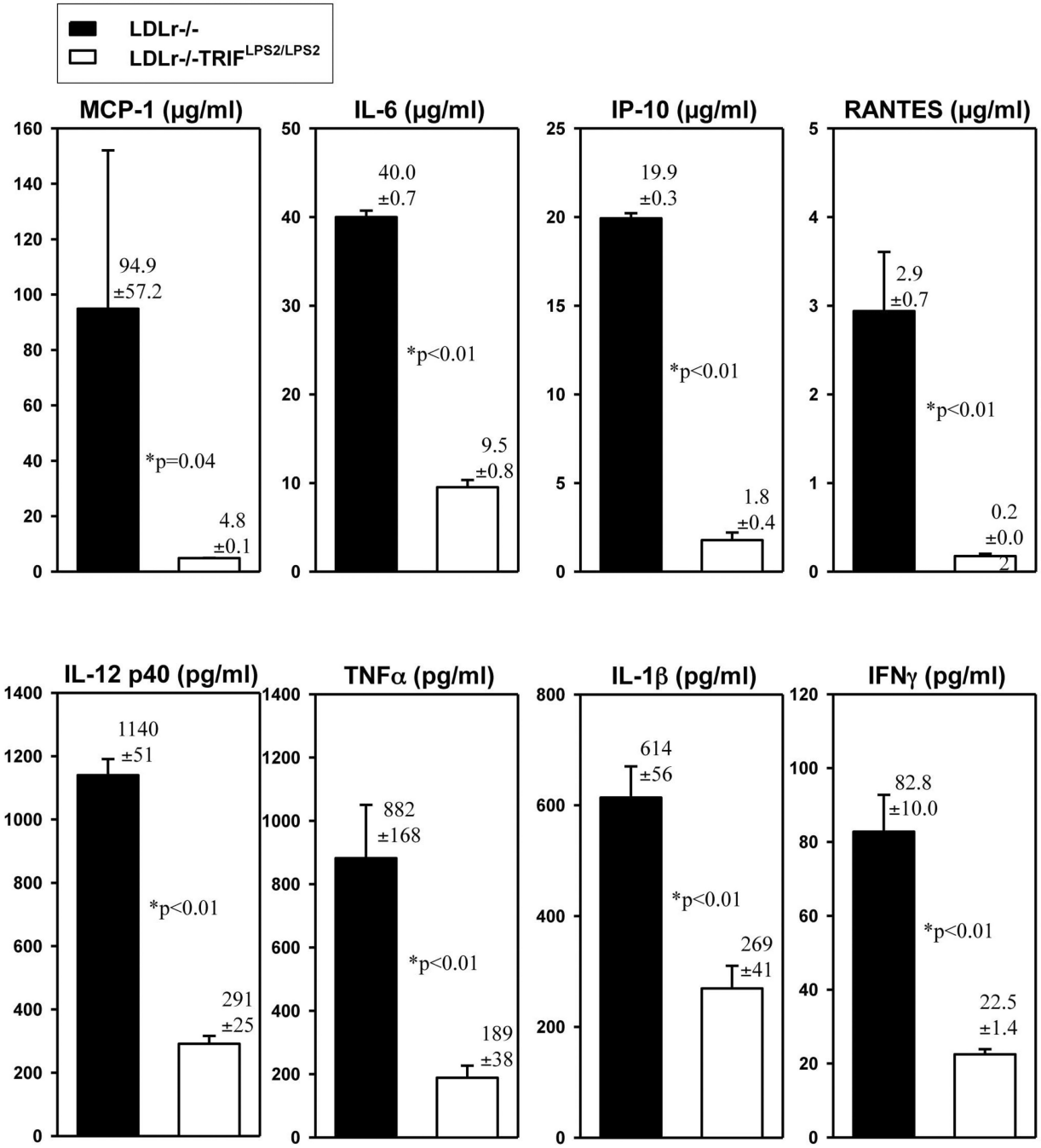

Figure 2. Cytokines Secreted by Resident Peritoneal Mϕ Obtained from HFD-Fed Mice

Cohorts of male LDLr−/− (n=8) or LDLr−/−TRIF$^{LPS2/LPS2}$ (n=13) mice were fed the HFD for 6 wks. Peritoneal Mϕ were harvested, plated at identical densities, and cultured overnight. Supernatants were collected and assayed for multiple cytokines by Luminex assay. Cytokines from both MyD88 (MCP-1, IL-6, IL-12p40, TNFα, top panel) and TRIF (IL1-β, IP-10, RANTES, IFNγ, bottom panel) pathways were examined.

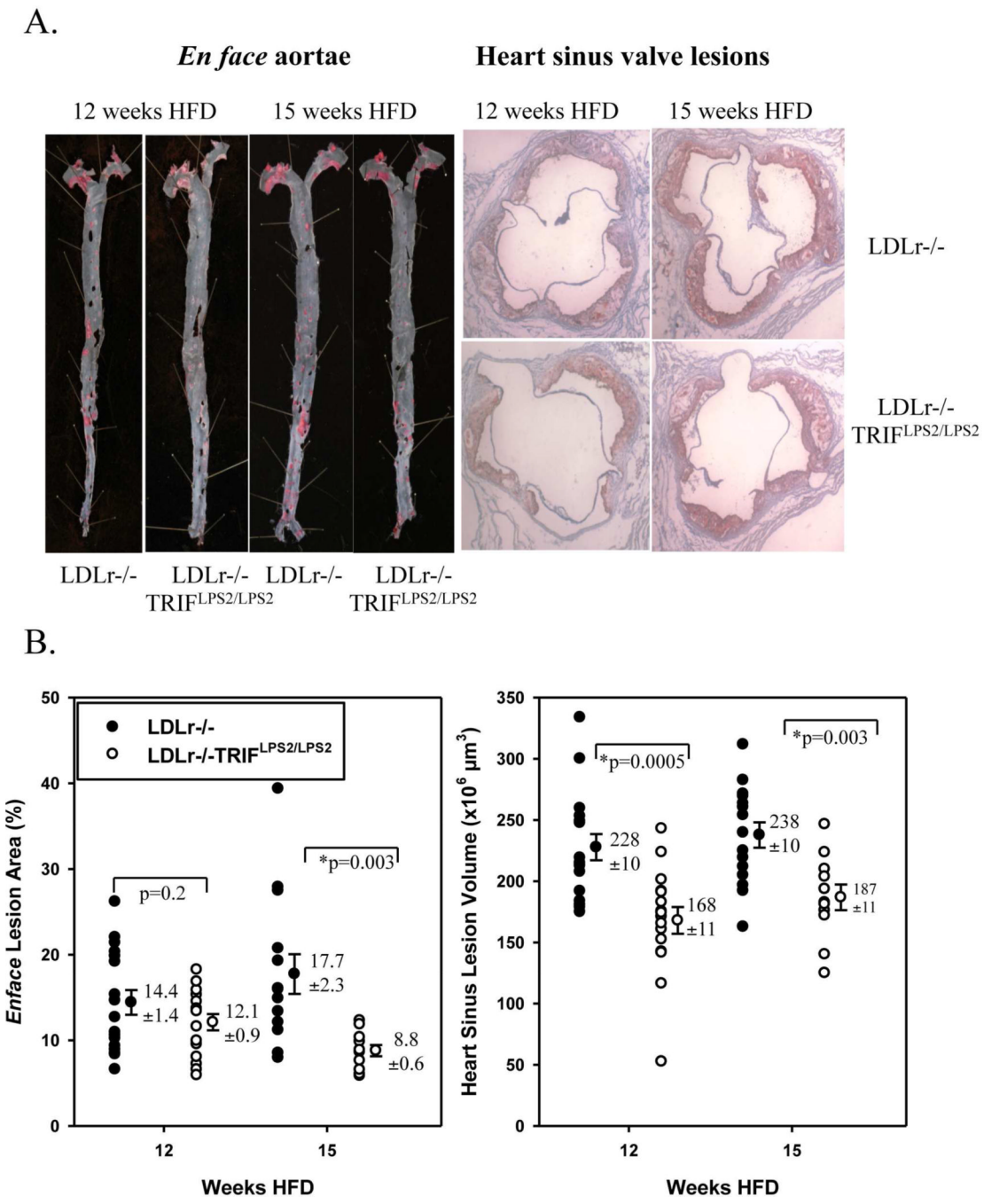

Figure 3. Atherosclerosis in LDLr−/−TRIF$^{LPS2/LPS2}$ Mice

Representative aortae (left) and heart sections (right) from each group are shown in (A). Lesion is stained with Sudan IV (aortae) or Oil Red O (hearts). Quantitation of lesion burden is shown in (B). Aortic lesion area (left) was calculated as a percent of total aortae surface area covered by lesion. Heart sinus valve lesion volume (right) was calculated from an integration of lesion area in cross sections from the proximal 500 µm of the sinus.

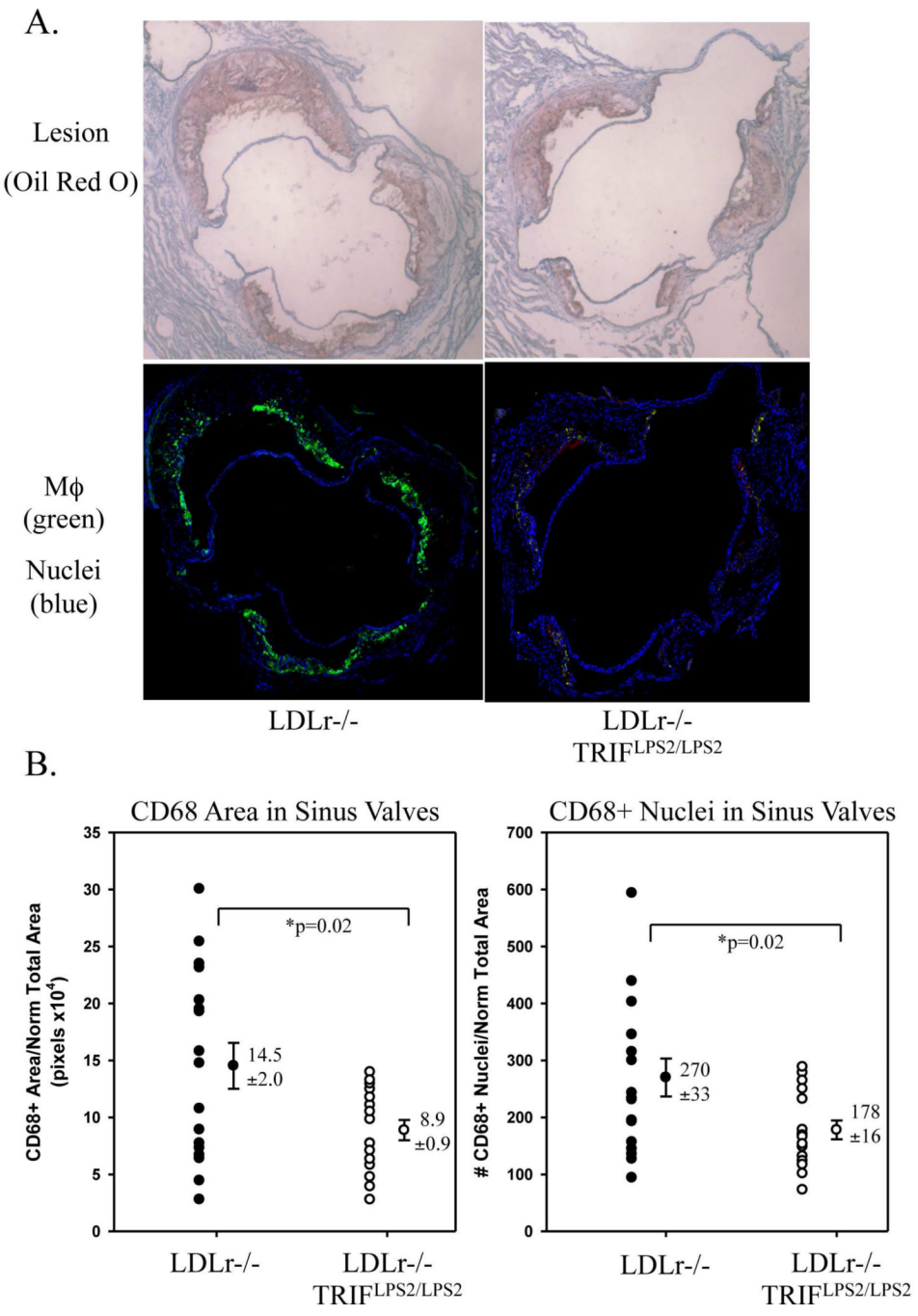

Figure 4. CD68-Positive Staining of Mϕs in Heart Sinus Valves

Serial sections from hearts stained with Oil Red O (A, top panel) were selected for staining of Mϕ (anti-CD68) and nuclei (DAPI) (A, bottom panel). CD68+ area (left) and number of CD68+ cells that colocalized with DAPI (right), normalized to the total valve area, is shown in (B).

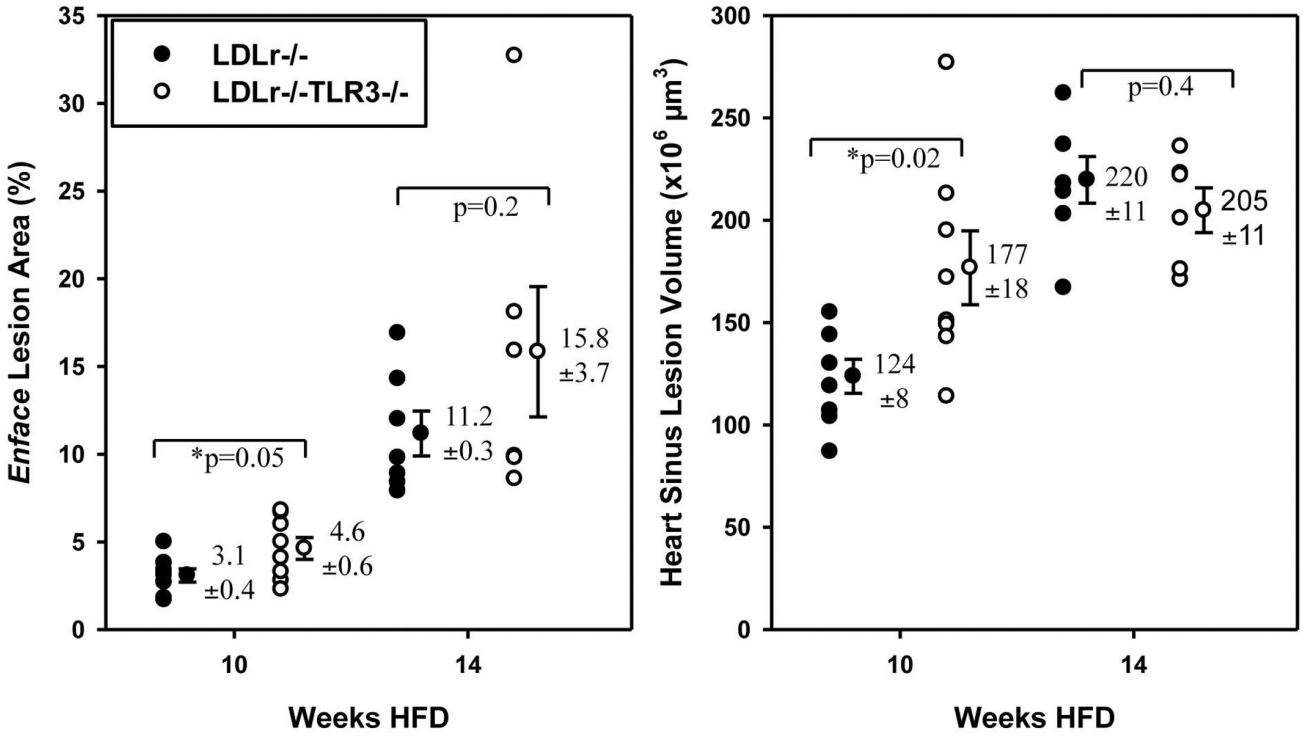

Figure 5. Atherosclerosis in LDLr−/−TLR3−/− Mice

Aortic lesion area (left) was calculated as a percent of total surface area covered by lesion (Sudan IV). Heart sinus valve lesion volume (right) was calculated from an integration of lesion area in cross sections from the proximal 500 μm of the sinus (Oil Red O staining).